Charge imbalance observed in voltage-biased superconductor–normal tunnel junctions

R. Yagi
Department of Quantum Matter, Graduate School of Advanced Sciences of Matter (ADSM), Hiroshima University, Higashi-Hiroshima, Hiroshima, 739-8530, Japan
(Received 7 February 2006; published 7 April 2006)

We have studied the tunneling current of a superconductor-insulator-normal tunnel junction connected to a nonequilibrium superconductor in which nonvanishing charge imbalance is present, by injection experiments using multiterminal devices fabricated with electron beam lithography. We found that the tunneling current could be separated into excess current, due to charge imbalance, and normal current, which showed clear and different dependences on the bias voltage, as expected from the theory of charge imbalance [M. Tinkham, Phys. Rev. B **6**, 1747 (1972)]. We also found in the analysis of the normal current that nonequilibrium distributions were created in the normal electrode; they were presumably caused by excitation due to hot electrons that tunneled from the nonequilibrium superconductor.

DOI: 10.1103/PhysRevB.73.134507 PACS number(s): 74.40.+k, 74.50.+r, 74.78.−w

Nonequilibrium electron systems are of the great interest these days for fundamental physics and for their potential applications. Nonequilibrium measurements can shed light on the hidden features of electrons in equilibrium. An example is the charge imbalance, the quasiparticle charge accumulation in superconductors.[1,2] The quasiparticles have two distinct features, electronlike or holelike particles, whose charge polarity is determined by the sign of $|k|-|k_F|$, where k is the wave vector of the quasiparticle and k_F is the Fermi wave vector. These features are hardly observed since the charge densities are identical in an equilibrium state. However, in a nonequilibrium state created by tunneling injection, the density can be unbalanced depending on the polarity of the injected charge. This phenomenon, charge imbalance, has been studied in terms of the relaxation time and resistance enhancement in phase slip centers and single junctions,[3–10] by measuring the chemical potential using the current balance method (CBM) involving a superconducting quantum interference device.[3–10] However, the behavior of the tunneling current of a junction in contact with a nonequilibrium superconductor has not been explored in isolation because the CBM limits the measurement to zero bias voltages. In this paper, we studied the issue by measuring the voltage-current characteristics.

The charge imbalance Q^* is the net charge density contributed by electron- and holelike quasiparticles and is given by $Q^*=2N(0)\int_\Delta^\infty(\delta f_{k>}-\delta f_{k<})dE$ with $\delta f_{k>}$ and $\delta f_{k<}$ being the distributions of electron- and holelike quasiparticles, $N(0)$ is the density of states at the Fermi level in the normal state, and Δ is the superconducting energy gap. The tunneling current of a voltage-biased superconductor-insulator-normal (SIN) junction connected to a nonequilibrium superconductor is the sum of the excess current δI, reflecting the charge imbalance, and the normal current I_n, which is similar to that widely observed in a SIN junction connected to an equilibrium superconductor. The excess current is independent of the bias voltages and is given by $\delta I=(G_{\rm nn}Q^*)/[2eN(0)]$ where $G_{\rm nn}$ is the junction conductance in the normal state.[1,2] The nonvanishing current appears even at a zero junction voltage if the populations of the electron- and holelike quasiparticles differ. The normal current, on the other hand, is dependent on the bias voltage and is determined by the distribution function $g(E)$ of an electron in the normal electrode of a SIN junction. It is given by the same formula as for the equilibrium state,

$$I=(G_{\rm nn}/e)\int_\Delta^\infty \pi(E)[g(E-eV)-g(E+eV)]dE \qquad (1)$$

where $\pi(E)$ is the normalized BCS density of states.[1,2]

To observe quasiparticle transport under finite bias voltage, we performed measurements using the device shown in Fig. 1. The device consisted of a narrow superconducting wire of aluminum and several $Al/AlO_x/Au$ junctions. The SIN junctions served as injectors and detectors of quasiparticles. Small junctions were fabricated using electron beam lithography and a shadow evaporation technique. The top and bottom electrodes of the junction were formed by using gold and aluminum. Tunnel barriers were formed by thermally oxidizing the aluminum surface. We selected a device whose junction resistances were between 5 and 10 kΩ. The measured superconducting energy gap of aluminum was 220 μeV at $T=70$ mK, which agreed with the BCS gap es-

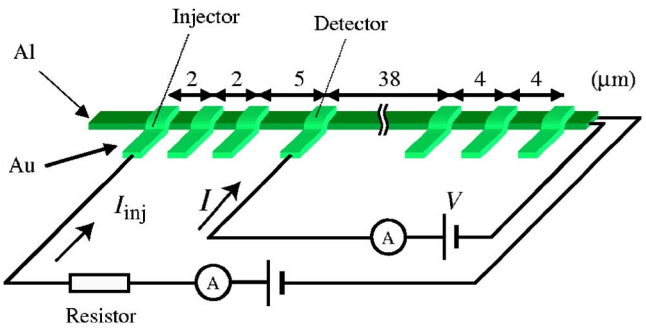

FIG. 1. (Color online) Schematic drawing of device structure. The device consisted of narrow aluminum superconducting wire (0.13 μm wide) on which several $Al/AlO_x/Au$ junctions were grown. Junction area was about 0.017 μm^2. Al and Au film thicknesses were 25 and 35 nm.

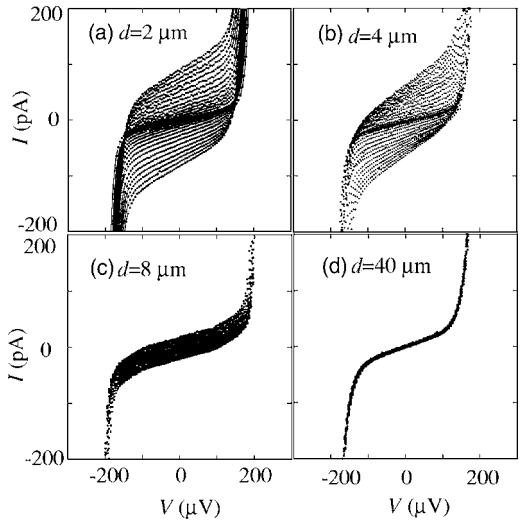

FIG. 2. Voltage-current characteristics of detector junction. Distance between detector and injector was (a) 2, (b) 4, (c) 8, and (d) 40 μm. From bottom to top, injection current was varied from −56 to 60 nA in 4 nA steps. $T=70$ mK. Tunneling resistance of detector junction was 7 kΩ. Data shown without offset current for display.

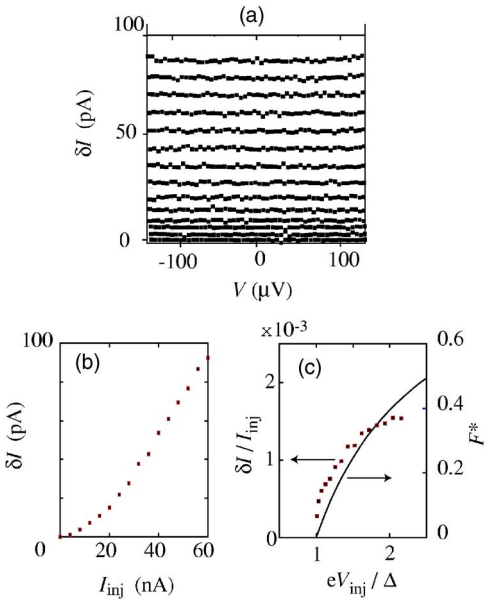

FIG. 3. (Color online) (a) Detector bias voltage dependence of excess current δI. From top to bottom, $|I_{\mathrm{inj}}|$ is decreased from 56 nA in 4 nA steps. $d=2$ μm. $T=70$ mK. (b) Dependence of δI on I_{inj} at $V=0$ V. (c) $\delta I/I_{\mathrm{inj}}$ vs normalized injection voltage V_{inj}. Also shown is V_{inj} dependence of F^*.

timated from $T_c=1.5$ K. Our aluminum film contained a small amount of oxygen, which caused a slightly higher T_c than the bulk. We have measured voltage-current characteristics in a temperature regime well below the T_c to suppress the quasiparticle current due to thermal excitation, which masks the detection of the excess current. The device was cooled to about 70 mK using a dilution refrigerator. The device was mounted on a rf-tight copper box thermally connected to a mixing chamber. The signal leads were filtered using copper powder filters and low-pass filters to attenuate external electric noise. The dc voltage-current characteristics were measured with a battery-powered voltage bias circuit and an ammeter.

Figure 2(a) shows the voltage-current characteristics of a detector junction connected to a superconducting wire into which quasiparticles were injected at a junction located 2 μm away from the detector. The I_{inj} was varied from −56 to 60 nA. The rapid increase in current at about ±180 μeV stems from the bias voltage approaching the superconducting energy gap 220 μeV. The *V-I* characteristics, as shown in Fig. 2, shifted gradually to an upper or lower position from the center with increasing magnitude of injection current. At $V=0$ V, for example, the nonvanishing current increased monotonically from −86 to 92 pA with increasing injection current from −56 to 60 nA. The magnitude of the current was approximately asymmetric with the injection current. This indicates that the observed phenomenon was nonlocal and was associated with the transport of nonequilibrium quasiparticles. This implies the existence of excess current possibly arising from a charge imbalance created by the injection in the superconducting wires.

The magnitude of charge imbalance should attenuate as the distance between the injector and detector increases, since the injected quasiparticles approach an equilibrium state as electrons and phonons interact while diffusing in the wire. Figures 2(b)–2(d) are similar measurements with different d ($d=4$, 8, and 40 μm). The range of the injection current was maintained the same as that used in Fig. 2(a). The magnitude of the excess current for the same I_{inj} diminished as d increased. For $d=40$ μm it was less than 1 pA, the minimum resolution of the current meter. Assuming that the excess current decayed exponentially in space, we estimated the relaxation length to be about 3.8 μm. These values are close to those obtained with a larger device structure and at much higher temperatures but well below T_c.[9]

In Figs. 2(a)–2(d) we noticed a characteristic of the normal current: the differential conductance at around a zero bias voltage increased monotonically with increasing magnitude of injection. We also recognized that the shape of the *V-I* characteristics was symmetric with the injection current if the excess current was subtracted. The current dependence on the bias voltages reflects the electron distribution $g(E)$ in the normal electrode. Thus, the observed changes in the shape of the *V-I* characteristics directly stem from the changes in $g(E)$ due to injection. The symmetric response of the shape of the *V-I* characteristics suggested that $g(E)$ was presumably determined by the magnitude of the energy transferred to the normal electrode by the nonequilibrium quasiparticles. This would be supported by the d dependence. Variations in *V-I* characteristics against I_{inj} were hardly visible in the data with $d=40$ μm, for example, where excess current was not discernible.

We extracted the excess current and the normal current from the *V-I* characteristics using their different responses to the polarity of the injection current. The excess current was an antisymmetric function of injection current, while the normal current was a symmetric function. Figure 3(a) shows the V dependence of the excess current obtained by the differ-

ence in current data at the same bias voltages for I_{inj} and $-I_{inj}$. Figure 3(a) clearly shows excess current in a voltage-biased junction whose magnitude is approximately unchanged with different bias voltages.

Other evidence for the excess current can be seen in the detailed response of the excess current to the injection. The tunneling injection creates electron- and holelike quasiparticles with a probability dependent on the injection voltage. At low voltages close to the superconducting energy gap, the creation of the charge imbalance is suppressed since electron- and holelike quasiparticles are created equally. With increasing injection voltage, the suppression vanishes. Figure 3(b) shows the I_{inj} dependence on the excess current. Suppression of the excess current in the small-injection-current regime ($I_{inj}<20$ nA) was visible. Figure 3(c) shows the behavior of $\delta I/I_{inj}$ against the injection voltage. Suppression of $\delta I/I_{inj}$ was clearly visible near the gap voltage. The magnitude of the charge imbalance was proportional to the injection current and to the efficiency F^* associated with the probability to create charge imbalance, which is dependent on the injection voltage. Here,

$$F^* = \frac{\int_\Delta^\infty \pi(E)^{-1}[f(E-eV_{inj}) - f(E+eV_{inj})]dE}{\int_\Delta^\infty \pi(E)[f(E-eV_{inj}) - f(E+eV_{inj})]dE} \qquad (2)$$

is a monotonically increasing function of the injection voltage that increases from zero at $V_{inj}=\Delta/e$ to unity for large Δ/e values.[11] Due to F^*, the excess current was considerably suppressed at around $V_{inj}=\Delta/e$; the decrease was more than that expected from the decrease in injection current. This explains the data shown in Fig. 3(c); the excess current was suppressed at small I_{inj} when the injection voltage was close to the energy gap. The discrepancy between the theory and experiment might be due to energy relaxation of the injected quasiparticles. Clarke and Paterson studied the injection voltage dependence of the chemical potential near T_c using the current balance method.[4]

Here, we compare the magnitude of the measured excess current with the theoretical estimate. The charge imbalance created at the injector reaches the detectors by quasiparticle diffusion. If we considering a steady one-dimensional diffusion in a long superconducting wire and a constant relaxation time, Q^* is given by the solution of the diffusion equation $D\frac{d^2Q^*}{dx^2} - Q^*/\tau_{Q^*}=0$, where D is the diffusion constant and τ_Q^* is the relaxation time. If a charge imbalance is created by injection at $x=0$, the end of the wire, Q^* at a distance x from the injector is $Q^*=(\lambda_{Q^*}I_{inj}F^*/eDS)e^{-x/\lambda_{Q^*}}$, where S is the cross-sectional area of the wire and $\lambda_{Q^*}=\sqrt{D\tau_{Q^*}}$ is the relaxation length. Using experimental parameters for λ_Q, I_{inj}, V_{inj}, and D, we estimated the excess current $\delta I=G_{nn}Q^*/2eN(0)$ to be 91 pA for $I_{inj}=60$ nA and $d=2$ μm. Here, we used the density of states for aluminum for one spin orientation, $N(0)=1.05\times10^{47}$ states/J m^3,[12] $F^*=0.43$ calculated for V_{inj} using Eq. (2), $D=5.2\times10^{-3}$ m^2/s obtained from the normal-state resistivity of aluminum at $T=4.2$ K, and the measured

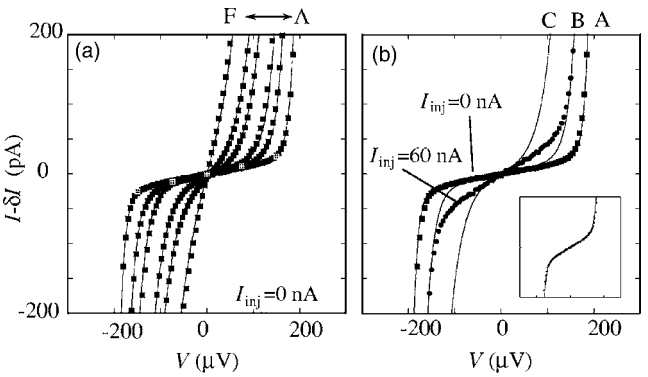

FIG. 4. (a) *V-I* characteristics of detector junction (without injection) for different temperatures. Solid squares represent measured data. Temperatures of curves *A* to *F* were 0.07, 0.10, 0.13, 0.20, 0.31, and 0.47 K. Simulated results were best fits when temperatures of the Fermi distribution function were 0.10, 0.17, 0.21, 0.29, 0.34, and 0.43 K (solid lines). We included parallel Ohmic conductance of 6.7 MΩ to reproduce *V-I* characteristics. (b) *V-I* characteristics of normal current for same junction. Squares represent measured data without injection. Normal current was obtained by extracting excess current from measured current. Circles represent measured data with $I_{inj}=60$ nA ($d=2$ μm). Solid lines represent simulated data assuming that $g(E)$ is a Fermi function. Temperatures of simulated curves *A* to *C* were 0.10, 0.18, and 0.28 K. Inset is line of best fit to measured data with $I_{inj}=60$ nA by experimental formula with $\alpha=0.0025$, $T_1=0.18$ K, and $T_2=1.6$ K.

$\lambda_{Q^*}=3.8$ μm. The calculated result agreed well with the measured value of $\delta I=92$ pA.

The relaxation time was not a directly measurable quantity in this experiment. However, we estimated it from λ_{Q^*} to be 2.8×10^{-9} s, which is approximately of the same order of magnitude as the value found in an experiment performed at a much higher temperature but well below T_c.[6,9] This seems to contradict the theoretical prediction that τ_{Q^*} arising from phonons[13] increases with decreasing temperature. We speculate that the measured τ_{Q^*} was mostly due to elastic scattering with the gap anisotropy,[2] which was not enhanced at low temperatures, because the measured τ_Q was about two orders of magnitude smaller than the theoretical estimation for phonons.[13]

Next we turn attention to the normal current. The shape of the *V-I* characteristics of the normal current varied depending on I_{inj} and d, as shown in Figs. 2(a)–2(d). As shown in Eq. (1), the local electron distributions $g(E)$ in the normal electrode are responsible for the changes in the *V-I* characteristics. The change in $g(E)$ is associated with power dissipation due to quasiparticle injection. Detailed inspection of the *V-I* characteristics revealed that $g(E)$ was given by the Fermi function without injection and that, with injection, $g(E)$ deviated from the Fermi function because of hot electrons created. We plotted the *V-I* characteristics with $I_{inj}=0$ nA for different temperatures, as shown in Fig. 4(a). We found that experiment was simulated fairly well by calculations assuming $g(E)$ to be the Fermi function. We plotted the *V-I* characteristics with and without injection measured at the lowest temperature, as shown in Fig. 4(b). In contrast to the good agreement between the experimental and simulated

data for $I_{inj}=0$ nA (curve *A*), data with $I_{inj}=60$ nA showed poor agreement. Curves *B* and *C* are simulations that could best fit the experimental data around a zero bias and higher voltages. In principle, the distribution might be determined by deconvoluting the *V-I* characteristics. However, we could not obtain sufficient accuracy because of the current above the gap voltages being considerably larger than the excess current. Alternatively, we estimated the nonequilibrium distribution using an experimental formula, $g(E)=(1-\alpha)f(E,T_1)+\alpha f(E,T_2)$, that included the hot-electron effect in the second term. Here, $f(E,T)$ is the Fermi function, and α, T_1, and T_2 ($|\alpha|\ll 1, T_1<T_2$) are the fitting parameters. The fact that the simulated *V-I* characteristics reproduced the measured *V-I* characteristics [inset of Fig. 4(b)] would suggest the presence of hot electrons in the normal electrode at the vicinity of the junction.

As seen in the *d* dependence shown in Figs. 2(a)–2(d), the normal current was possibly related to the density of the nonequilibrium quasiparticles at the detector. The electrons in the normal electrode could be excited by quasiparticle tunneling at the detector since the quasiparticles tunneling from the superconductor to the cold normal electrode gave the normal electrode the energy of at least Δ on average. The steady tunneling of quasiparticles would create a nonequilibrium electron distribution in the normal electrode at the vicinity of the junction. This might be related to the nonequilibrium distribution observed in mesoscopic metal wires.[14] Phonons created in energy relaxation or recombination of quasiparticles could excite the electrons in the normal electrode. However, we speculate that this is not a major contributory factor. We think that such a large difference in the *d* dependence in the scale of interest (40 μm) would not result from the phonons, considering its long mean free path of the order of 200 μm (Ref. 15) and the weak electron-phonon coupling which is proportional to T^5 at low temperatures.[16]

To date, studies of the tunnel current in contact with nonequilibrium superconductors have not been made experimentally. The existing experiment assumed implicitly that the excess current is unchanged with varying bias voltage. In our experiment, we clarified that the current is composed of the sum of the excess current due to charge imbalance and the normal current, as predicted in the theory of charge imbalance. We have shown this by the essential difference in the symmetry in the injection current used to create charge imbalance. Tinkham's theory assumes that the normal electrode is an ideal electron reservoir whose electron distribution follows the Fermi function. However, in actual experiments, the electron temperature in the normal electrode is expected to increase because of quasiparticle injection. In addition, the electrons in the electrode can be in nonequilibrium particularly at low temperatures. Thus, the assumption is valid for small magnitudes of charge imbalance or for rather high temperatures. For other cases, the normal current should be calculated using the actual distributions in the normal electrode.

The CBM is capable of determining the excess current of a SIN junction in contact with a nonequilibrium superconductor. Voltage is applied to the junction to eliminate the total current using feedback from a superconducting quantum interference device SQUID voltmeter to detect the voltage across the detector junction. This method is effective for the high-temperature regime and small magnitudes of charge imbalance, where the voltage signal, the product of the zero-bias conductance, and the excess current are small. This is the case for the temperatures near T_c. In the opposite case, the CBM is not effective for two reasons: the nonlinearity of the voltage-current characteristics and nonequilibrium electron distributions in the normal electrode. This would be a serious problem, in particular, at low temperatures, in which quasiparticle resistance increases almost exponentially and nonlinear behavior near the gap voltage is significant. At the low-temperature limit, the voltage to be measured by the CBM would be about the superconducting energy gap for nonvanishing excess current regardless of its magnitude. Moreover, the nonequilibrium distribution in the normal electrode influences the zero-bias conductance of the junction, which is required to analyze the CBM result: unless one measures the conductance for each injection current, what was measured by CBM might have an error in the estimation of the magnitude of the charge imbalance. Therefore, our method described here favors measurements at temperatures much lower than T_c.

The author thanks Y. Ikebuchi for technical support in this experiment. This work was supported in part by a Grant-in-Aid for Scientific Research (No. 140212) and a Grant-in-Aid for COE research (No. 13Ce2002) of the Ministry of Education, Culture, Sports, Science and Technology of Japan.

[1] M. Tinkham and J. Clarke, Phys. Rev. Lett. **28**, 1366 (1972).
[2] M. Tinkham, Phys. Rev. B **6**, 1747 (1972).
[3] J. Clarke, Phys. Rev. Lett. **28**, 1363 (1972).
[4] J. Clarke and J. L. Paterson, J. Low Temp. Phys. **15**, 491 (1974).
[5] G. J. Dolan and L. D. Jackel, Phys. Rev. Lett. **39**, 1628 (1977).
[6] C. C. Chi and J. Clarke, Phys. Rev. B **19**, 4495 (1979).
[7] T. R. Lemberger and J. Clarke, Phys. Rev. B **23**, 1088 (1981).
[8] T. R. Lemberger and Y. Yen, Phys. Rev. B **29**, 6384 (1984).
[9] H. J. Mamin, J. Clarke, and D. J. Van Harlingen, Phys. Rev. B **29**, 3881 (1984).
[10] M. Johnson and R. H. Silsbee, Phys. Rev. Lett. **58**, 2806 (1987).
[11] M. V. Moody and J. L. Paterson, J. Low Temp. Phys. **34**, 83 (1979).
[12] We estimated the density of state of aluminum from the specific heat data of C. Kittel, *Introduction to Solid State Physics* (John Wiley & Sons, New York, 1976), p. 166.
[13] S. B. Kaplan, C. C. Chi, D. N. Lagenberg, J. J. Chang, S. Jafarey, and D. J. Scalpino, Phys. Rev. B **14**, 4854 (1976).
[14] H. Pothier, S. Gueron, N. O. Birge, D. Esteve, and M. H. Devoret, Phys. Rev. Lett. **79**, 3490 (1997).
[15] The low-temperature mean free path of phonons in a Si substrate was estimated by extrapolating the data in R. Gereth and K. Hubner, Phys. Rev. **134**, A235 (1964).
[16] F. C. Wellstood, C. Urbina, and J. Clarke, Phys. Rev. B **49**, 5942 (1994).